International Journal of Microwave and Wireless Technologies, 2015, 7(3/4), 459–467. doi:10.1017/S1759078715000641

RESEARCH PAPER

Radar micro-Doppler of wind turbines: simulation and analysis using rotating linear wire structures

OLEG A. KRASNOV AND ALEXANDER G. YAROVOY

A simple electromagnetic model of wind-turbine's main structural elements as the linear wired structures is developed to simulate the temporal patterns of observed radar return Doppler spectra (micro-Doppler). Using the model, the micro-Doppler for different combinations of the turbines rotation frequency, radar pulse repetition frequency, and duration of the Doppler measurement interval are analyzed. The model is validated using the PARSAX radar experimental data. The model ability to reproduce the observed Doppler spectra main features can be used for development of signal-processing algorithms to suppress the wind-turbines clutter in modern Doppler radars.

Keywords: Radar, Electromagnetic simulation, Micro-Doppler, Wind turbines

Received 31 October 2014; Revised 13 March 2015; Accepted 17 March 2015; first published online 1 June 2015

I. INTRODUCTION

Attention to "green" energy sources results in fast spreading of wind turbines, which convert wind energy into electricity. Efficiency of such turbines is directly proportional to their sizes (up to 70–90 m blades length) and heights (up to 100–200 m). Wind farms with such turbines already influence the existing radar systems for civil and military surveillance, air-traffic control, and weather radar networks, as radar signal scattering from turbines results in clutter-like interference with specific dynamics that degrade radar's functionality, the ability to detect targets and estimate their characteristics [1, 2]. The rotating blades of wind-turbines move with high azimuthal velocity and produce strong clutter with wide continuous Doppler spectra, which hide targets and disturb their estimated parameters. Development of new algorithms for the suppression of such clutter is a challenging research topic and one of the main tasks for the radar community [2, 3].

To support such algorithms development and provide better understanding of radar returns from wind turbines we propose a very simple model, which represents the main structural elements of wind turbines (mainly blades) as linear wire structures. Despite of its over simplification, the model still predicts correctly the temporal behavior of Doppler radar spectral observables in the far-field region. It can be used to extract the major parameters of wind turbines and for initial testing of clutter suppression algorithms, which are using specific features of wind-turbines' micro-Doppler or temporal-Doppler patterns.

The paper is organized as follows: Section II describes briefly the developed electromagnetic (EM)-model of wind turbines, which is used for further simulations. Section III presents the simulation results for a few basic structures and, for one practical case, compares simulations results with real radar observations by the *S*-band PARSAX polarimetric Doppler radar. Section IV discusses the influence of the relation between the wind-turbine blades rotation frequency and the radar observation duration on the resulting Doppler spectra. Section V draws some conclusions and discusses further research directions.

II. RADIATION OF ROTATING LINEAR WIRED STRUCTURE

In order to simulate and analyze the spectral, temporal, and angular dependency of radar signals scattered from wind turbine, we assume that the turbine's blades can be modeled using very thin ($Ø \ll \lambda$) finite length linear wires. It is clear that such approximation is oversimplified for most the popular radar frequency bands, but it allows analytical derivation of the basic close-form solutions for the radar observables in the far-field region.

A) Basic relations for an infinitesimal dipole

The basic approach to estimate the EM field radiated by or scattered from a finite-size linear wire structure is to subdivide it into a number of infinitesimal dipoles of length dz' [4]. The electric and magnetic field components in the spherical

Microwave Sensing, Systems and Signals (MS3), Delft University of Technology, Delft, The Netherlands
Corresponding author:
O.A. Krasnov
Email: O.A.Krasnov@tudelft.nl

coordinate system of the field radiated by an infinitesimal dipole of length dz' positioned along the z-axis at z' (see Fig. 1) in the far field are given as [4]

$$dE_\theta \simeq j\eta \frac{kI_e(x', y', z')\, e^{-jkR}}{4\pi R} \sin\theta\, dz', \tag{1}$$

$$dE_r \simeq dE_\phi = dH_r = dH_\theta = 0, \tag{2}$$

$$dH_\phi \simeq j \frac{kI_e(x', y', z')\, e^{-jkR}}{4\pi R} \sin\theta\, dz', \tag{3}$$

where $I_e(x', y', z')$ is the electric current strength at the infinitesimal dipole, the wavenumber k is $k = 2\pi/\lambda$, η is the intrinsic impedance of propagation medium, and R is the distance from any point z' on the wire to the observation point, given by $R = \sqrt{r^2 + (-2rz'\cos\theta + z'^2)}$, where r is the distance from the center of coordinates to the observation point. The harmonic factor $e^{-j\omega t}$ in equations (1)–(3) and their derivatives are omitted.

Using the far-field approximation, when R can be replaced by $R \simeq r - z'\cos\theta$ for the phase terms and by $R \simeq r$ for the amplitude terms, equation (1) can be written as

$$dE_\theta = j\eta \frac{kI_e(x', y', z')\, e^{-jkr}}{4\pi r} \sin\theta\, e^{+jkz'\cos\theta} dz'. \tag{4}$$

A similar equation can be derived for the magnetic field component (3). As all other radiated field components are equal to zero (2), an infinitesimal dipole is a pure polarization-anisotropic object. For such an object the generation of cross-polarized components of (re-)radiated field completely defined by the orientation of the dipole in the polarization basis of the radar's antenna system. As soon as in this paper we study the temporal behavior of the Doppler spectra of rotating blades, we will exclude geometric depolarization from consideration, and analyze the case when the radar is placed in the rotation plane of the structure and causing polarization of the radar signals in the rotation plane only.

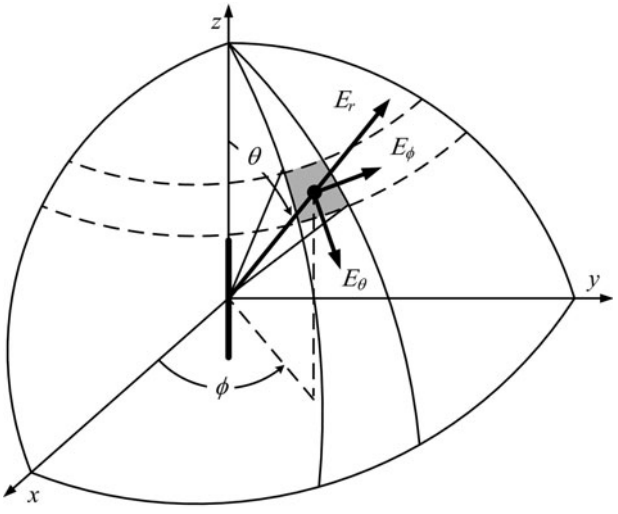

Fig. 1. The geometry of the components of the electric field, radiated by infinitesimal dipole (after [4]).

B) Radiated field of finite length linear wire structure

Summing up the contributions from all the infinitesimal elements over a wire structure with a length L one derives

$$E_\theta = \int_L dE_\theta = j\eta \frac{k\, e^{-jkr}}{4\pi r} \sin\theta \left[\int_L I_e(x', y', z')\, e^{jkz'\cos\theta} dz' \right]. \tag{5}$$

The radiated field is defined by two factors – the term outside the brackets is usually called as the *element factor* and the one within the brackets as the *space factor*. For analyzed linear wire structure, the element factor is defined as the field of a unit length infinitesimal dipole located at a reference point (the origin). In this study, we assume this point to be collocated at the center of the wind-turbine rotation. In general, this factor depends on the type of current and its direction. The space factor is a function of the current distribution along the linear wire structure.

If we assume that the wire structure is rotated, the elevation angle changes in time proportionally to the rotation frequency Ω as $\theta(t) = \theta_o + \Omega t$, and for the most practically important cases $\Omega \ll \omega$. This allows to simulate directly the scattered from rotating wire structure radar signals in time domain using equation (5) with following conversion to the Doppler frequency domain.

A combination of n linear wires produces the total scattered field as:

$$E_\theta = \sum_n \int_{L_n} dE_\theta = j\eta \frac{k\, e^{-jkr}}{4\pi r} \times \sum_n \sin\theta_n \left[\int_{L_n} I_e(x', y', z')\, e^{jkz'\cos\theta_n} dz' \right]. \tag{6}$$

In this equation, we assume that there is no EM coupling between different elements of analyzed wire structure. This assumption, which is not correct from pure electrodynamics point of view, allows us to keep the analysis of complex wire constructions simple and is still useful for the interpretation of experimental results.

In the case of monostatic radar, the single-scattered on every infinitesimal piece of wire field is defined by the induced current $I_{ind}(x', y', z')$, which is proportional to the tangential component of the incident radar signal's field. The phase of this field in every specific location can be defined using the phase shift of the incident field relatively to the selected at the distance r phase (and rotation) center of the wire structure. As result, the induced on a wire structure current defined as

$$I_{inc}(x', y', z') \sim E_\theta(r) \cdot \sin\theta \cdot e^{+jkz'\cos\theta}. \tag{7}$$

The resulting backscattered field is proportional to

$$dE_\theta^{BS}(\theta, z') \sim j\eta \frac{ke^{-jkr}}{4\pi r} E_\theta(r) \cdot \sin^2\theta \cdot e^{+j2kz'\cos\theta} dz'. \tag{8}$$

III. CASE STUDIES

In this section, we apply the model developed in the previous section to different rotated linear wire structures to simulate and analyze the amplitude Doppler spectrogram – the temporal pattern of the observed by radar Doppler spectrum. For presented cases in this paper, we simulated a Doppler radar with the operational wavelength 10 cm (*S*-band) that transmits with the pulse repetition frequency (PRF) 1 kHz the bursts of 128 pulses. Every such burst is used for the Doppler processing with zero-padding till 1024 samples for enhanced spectra representation. For the results presentation we selected the method of short-time Fourier transforms (spectrogram), which clearly demonstrates changes in the observed Doppler spectrum over time. In all presented cases the simulated wire structures rotate with rotation frequency $\Omega = 0.1$ Hz (rotation period 10 s) and the radar's line of sight is assumed to be parallel to the rotation plane (observation azimuth angle $\phi_o = 0^\circ$). We do not include in simulations the reflections from the supporting tower, keeping only (re-)radiated by rotating blades signals. It is clear that the reflection from stable in time wind-turbine tower adds strong zero-Doppler component to presented cases.

Changing the wire orientation angle according to the structure's rotation speed with time intervals, which are equal to radar pulse repetition interval, provide the initial radar signals for further Doppler processing.

A) Radiating long dipole antenna

To verify theoretically the model proposed and to create a reference for further analysis, we start with micro-Doppler simulation of a very long symmetrical dipole transmit antenna, which is fed at and rotates around its central point. In this case the current distribution along the wire is given by

$$I_e(x' = 0, y' = 0, z') = \hat{\mathbf{a}}_z I_0 \sin\left[k\left(\frac{l}{2} - |z'|\right)\right] \quad -l/2 \le z' \le l/2, \tag{9}$$

where I_o is the amplitude of the current in the feeding point. By substituting this equation into equation (5) and performing numerical integration one obtains the transmitted far-field patterns of such a dipole as a function of the changing in time orientation angle in the rotation plane. Comparison of the calculated radiation patterns for a finite-length dipole antenna [4] with their analytical representation was used for the numerical algorithm validation.

The computed Doppler spectrogram of the received signals in the rotation plane with the initial elevation angle $\theta_o = 0^\circ$ are presented in Figs. 2 and 3. The maximum Doppler shift appears at $\theta = \pm 90^\circ$, when the dipole becomes perpendicular to the observer's line of sight. The intensity of the zero-Doppler component strongly depends on the long dipole's side lobes patterns, which are defined by the relation of antenna length to wavelength. In case of $L = (n \pm 1/2)\lambda$ the presence of the broadside lobes results in complete suppression of the zero-Doppler signals.

B) Asymmetrical long wire as a radar reflector

In case when the rotation center coincides with one of the wire end, the resulting Doppler spectrogram is presented in Fig. 4. The maximal Doppler shift occurs when the rotated wire becomes perpendicular to the radar's line of sight and all

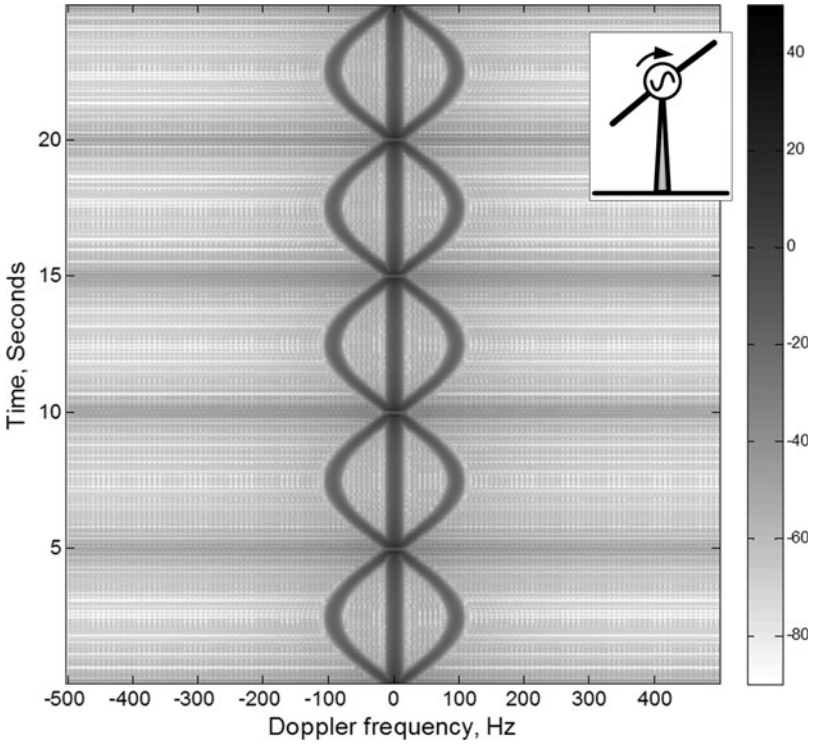

Fig. 2. Amplitude Doppler spectrogram (in dB) of the rotating symmetrical radiating dipole antenna with the total length $L = 300\lambda$, the rotation frequency $\Omega = 0.1$ Hz, and the initial elevation angle $\theta_o = 0^\circ$.

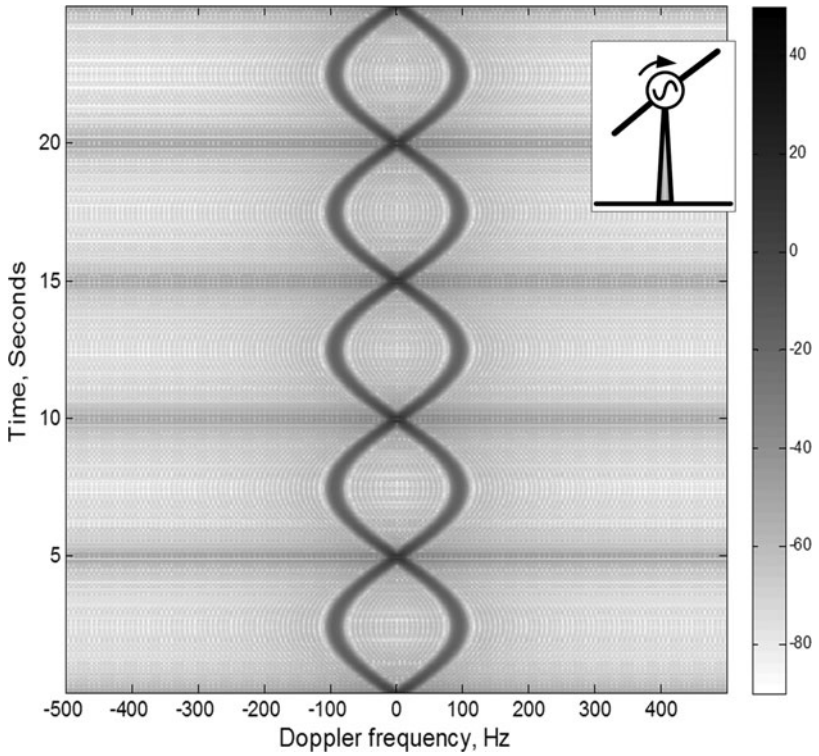

Fig. 3. Amplitude Doppler spectrogram (in dB) of the rotating symmetrical radiating dipole antenna with the total length $L = 300.5\lambda$, the rotation frequency $\Omega = 0.1$ Hz, and the initial elevation angle $\theta_o = 0^\circ$.

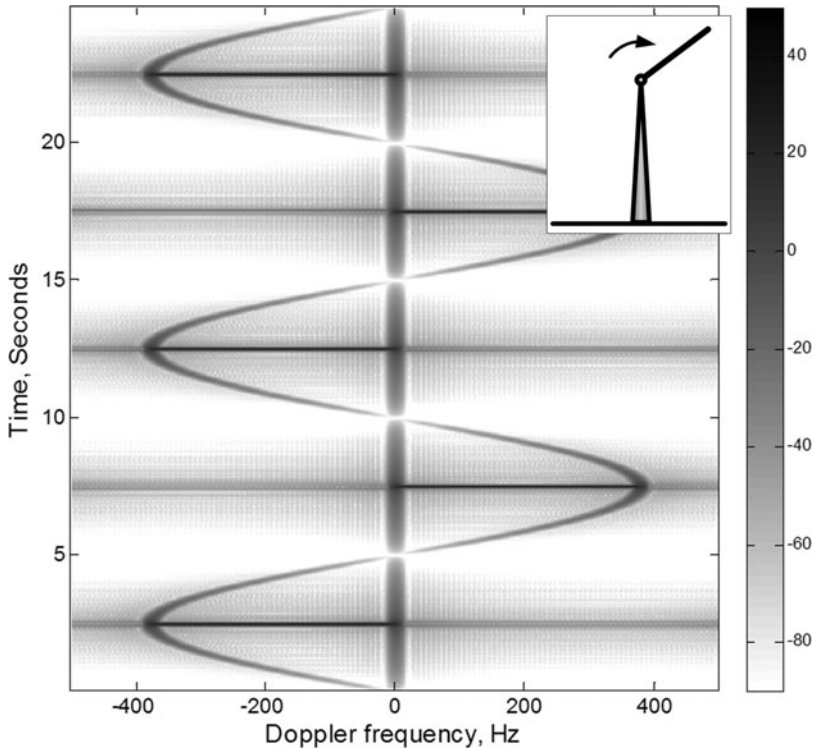

Fig. 4. Amplitude Doppler spectrogram (in dB) of a rotating asymmetrical linear wire with the length $L = 300\lambda$, the rotation frequency $\Omega = 0.1$ Hz, and the initial elevation angle $\theta_o = 0^\circ$ (the structure reflects radar signals in the rotation plane).

Doppler frequencies from zero till maximum value are presented in the spectrum with the same amplitude. Much lower amplitudes of temporal harmonic-like reflections are produces by the side lobes of reradiated by the wire field. The weakly modulated zero-Doppler reflections are presented for any length of the wire.

C) Symmetrical long wire as a radar reflector

The shift of the rotation center to the middle of the wire results in full symmetrization of the observed Doppler spectrum (Fig. 5). For the given example the total length of the wire structure is the same as in the previous asymmetrical case (Fig. 4), as result the maximum Doppler shift expectedly decreased in two times.

D) Wired model of a wind turbine with three blades

A combination of three linear wires, which are progressively shifted by 120° with respect to each other in the rotation plane, creates a simple wire model of typical high-efficient wind turbine.

The simulated temporal dependence of the micro-Doppler spectral pattern for such wire structure is presented in Fig. 6. It represents quite well the main feature of real Doppler spectrogram of wind turbines with three blades.

Now we apply proposed model for the detailed interpretation of the real radar measurements of the Enercon E82-2.3 MW wind turbine [5, 6] near Etten-Leur, the Netherlands. The micro-Doppler pattern (temporal Doppler spectrogram) of such turbine measured with the PARSAX S-band radar [7] is shown in the upper image in Fig. 7. For this a continuous LFM waveform with PRF 1 kHz and the bandwidth of 10 MHz was used. The Doppler spectrum pattern was calculated for sequential bursts of 128 sweeps using Hamming windowing without any noise and clutter suppression, and has been incoherently integrated over five range resolution elements to cover the most parts of wind-turbine construction.

In the turbine model with three-wires as described above the wires lengths of 82 m is used based on the available wind-turbine documentation [5, 6]. The blades rotation frequency ($\Omega = 0.03$ Hz) has been determined from the periodicity of the real radar spectrogram (upper image in Fig. 7). After the blades rotation frequency selection, the simulated observation azimuth (angle between radar's line of sign and blades rotation plane) has been determined using the matching of the maximum observed Doppler speed with maximum expected linear speed of the end point of blade for the given blade's length and rotation speed. This turning was necessary as soon as, unfortunately, for this observation case the ground-truth data about the orientation of the blades rotation plane were not available. To limit the dynamic range of simulated spectrogram the Gaussian noise with a level, defined from the signal-to-noise ratio of the real radar data, was injected into the model during the simulation.

The simulated micro-Doppler pattern is presented in the middle image in Fig. 7. To represent visible on the real radar spectrogram temporal widening of the main Doppler spread lines and some harmonic-like patterns every blade was presented in the model as electromagnetically independent combination of three parallel wires with different lengths.

To represent more details of the real micro-Doppler pattern a few different corrections of simulated wire structure have been done. Finally, we found the way to reproduce the exponentially like decreasing in time pattern, which is located on micro-Doppler spectrogram after the main Doppler spread line – as it is shown in bottom image in Fig. 7. In this simulation, each blade has been modeled as a bunch of wires, separated in orientation in 3°, and their lengths are decreasing with the parabolic law. The simulated and real micro-Doppler patterns looks quite similar, and the

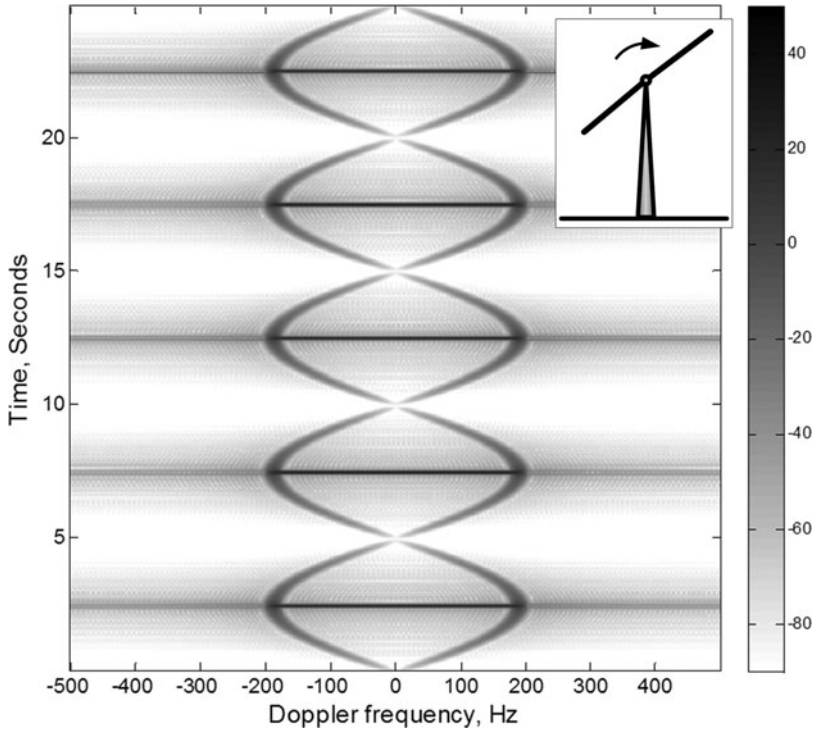

Fig. 5. Amplitude Doppler spectrogram (in dB) of a rotating symmetrical linear wire with the length $L = 300\lambda$, the rotation frequency $\Omega = 0.1$ Hz, and the initial elevation angle $\theta_o = 0°$ (the structure reflects radar signals in the rotation plane).

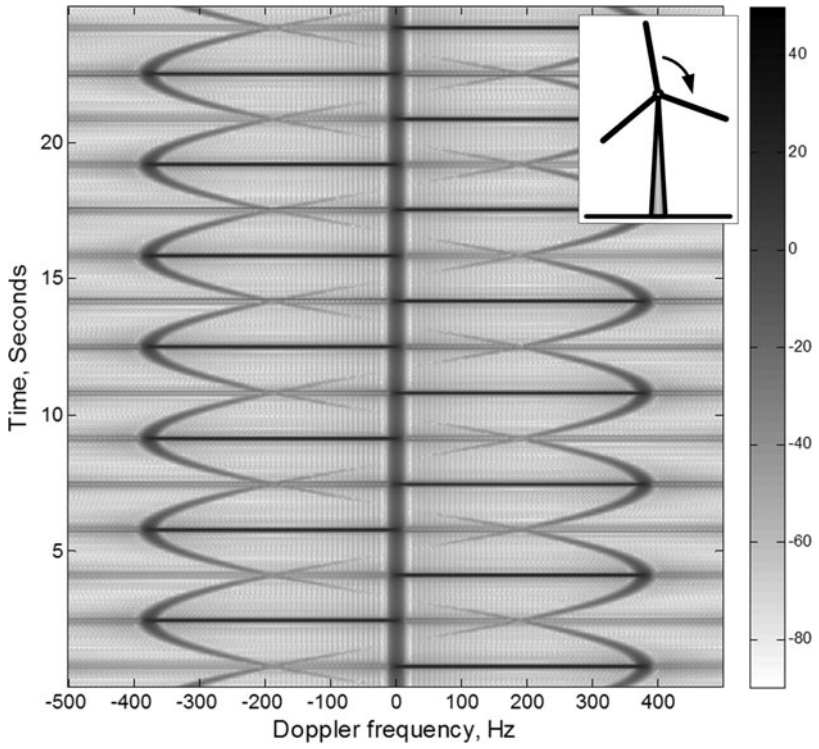

Fig. 6. Amplitude Doppler spectrogram (in dB) of a rotating structure with three linear wires with the length $L = 300\lambda$, progressively shifted in the rotation plane by 120°, the rotation frequency $\Omega = 0.1$ Hz, and the initial elevation angle $\theta_o = 0°$ (the structure reflects radar signals in the rotation plane).

resulting multi-wire structure also looks much more similar to the real turbine's blades.

V. ROTATION FREQUENCY AND DOPPLER SPECTRUM

The simple close-form representation of the scattered EM field in the proposed model gives a possibility to analyze analytically temporal behavior of the scattered signal. As soon as a radars measures the Doppler spectrum during some specific time interval Δt (the time on target, dwell time), it is interesting to study the influence of the relation between this observation time and radar target's rotation period on the measured Doppler spectrum.

In Section II, we assumed that as the linear wired structure rotates, the elevation angle changes in time proportionally to rotation frequency $\theta(t) = \theta_o + \Omega t$ and, for most practically important cases, $\Omega \ll \omega$. The dependence of the element factor in equation (5) from the elevation angle θ defines the amplitude harmonic modulation of the scattered in a specific direction field with the frequency Ω. Below we analyze the results of the harmonic phase modulation under the integral in the space factor in equation (5).

A) Slowly rotating objects

For the case of slowly rotating wire structure, when the radar observation time Δt is much shorter than rotation period ($\Omega \Delta t \ll 1$), from the known serial expansion [8]:

$$\cos\theta(t) = \cos(\theta_o + x) = \cos\theta_o - x\sin\theta_o - \frac{x^2}{2!}\cos\theta_o + \frac{x^3}{3!}\sin\theta_o + \cdots, \qquad (10)$$

where $x = \Omega t$, follows that

$$e^{jkz'\cos\theta(t)}e^{j\omega t} \approx e^{jkz'\cos\theta_o}e^{j(\omega - \Omega kz'\sin\theta_o)t}. \qquad (11)$$

The second term in the right part of the equality (11) can be seen as the classical Doppler shift, which depends on the wire structure's rotation frequency as well as the orientations and positions of integrated infinitesimal dipoles relatively to the center of rotation.

B) Fast rotating objects

As soon as the wire's rotation period becomes comparable with the radar observation interval, not only linear terms in the serial expansion (10) have to be taken into consideration, and this expansion becomes not convenient to use for the close-form analysis. In this case, we can use relation (9.1.4, [8])

$$e^{[(1/2)z(y-\{1/y\})]} = \sum_{k=-\infty}^{\infty} y^k J_k(z), \quad y \neq 0, \qquad (12)$$

where $J_k(z)$ are the Bessel functions of integer order k. Defining in equation (12) $y = e^{j\Omega t}$, assuming without loss of generality $\theta_o = 0$, and using the fact that $\cos x = \sin(x + \pi/2)$, we come to the following result

$$e^{jkz'\cos\Omega t}e^{j\omega t} = e^{j\omega t}\sum_{k=-\infty}^{\infty} e^{j(\pi n/2)}J_k(kz')\,e^{j\Omega kt}. \qquad (13)$$

This equation represents the symmetrical distribution of an infinite amount of harmonics around the center frequency, in many senses similar to the spectrum of the frequency-modulated with harmonic signal of frequency Ω. It means

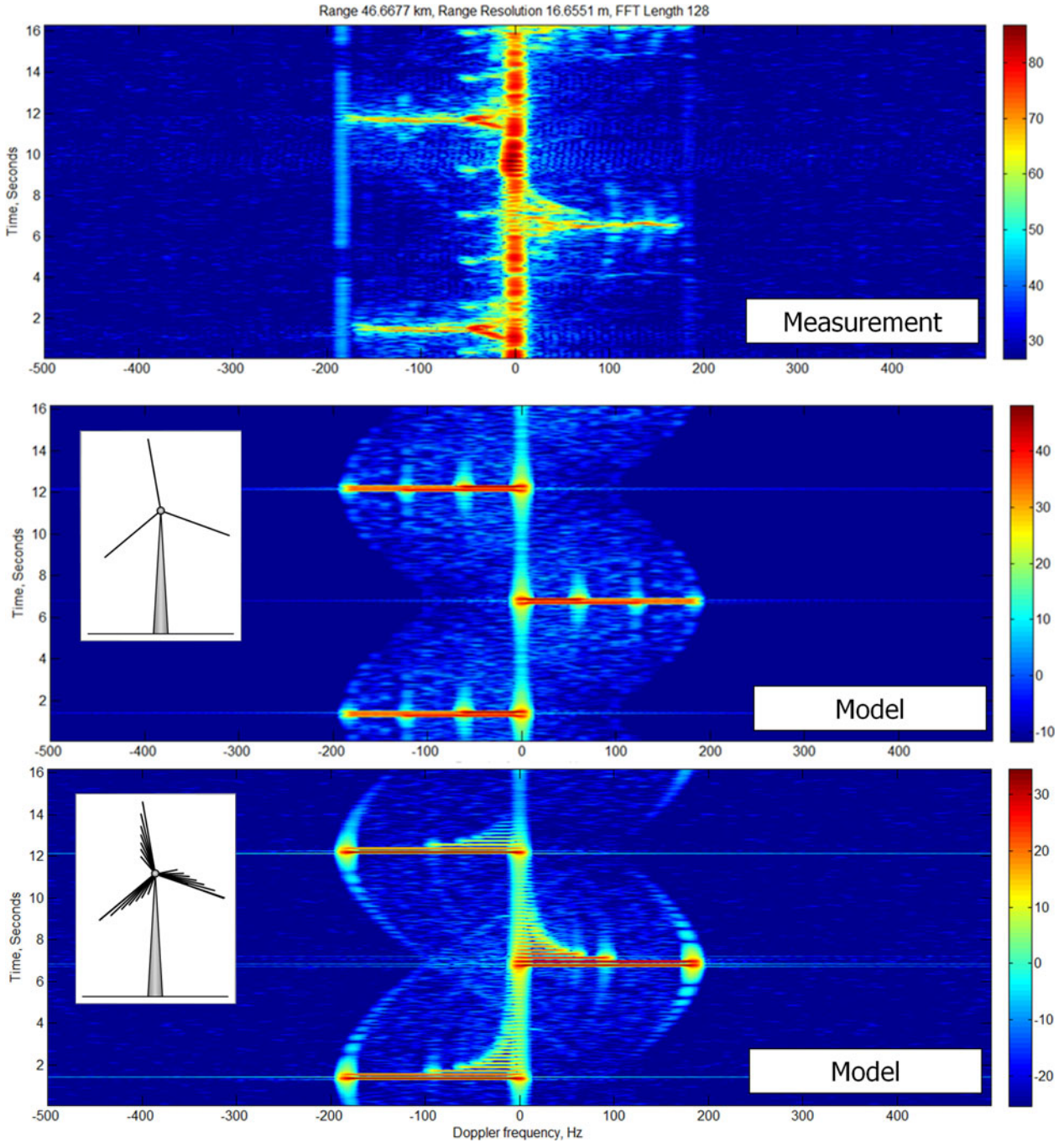

Fig. 7. Amplitude micro-Doppler pattern (amplitude Doppler spectrogram, in dB) of the Enercon E82-2.3 MW wind-turbine near Etten-Leur, the Netherlands: measured with the PARSAX *S*-band radar (top) and simulated on the base of proposed algorithm for the simple three parallel wires per blade structure (middle) and for more complex structure when every blade is modeled as a bunch of wires (bottom).

that in case of fast rotated objects or long radar observation time, when radar observation time becomes compatible or longer then the rotation period, the Doppler model of spectrum interpretation is not working anymore. An observer will measure the continuous symmetrical spectrum with separated by Ω harmonics.

C) Simulated examples

The three wires model of wind turbine has been used for simulation of spectrograms for cases with different relation between the wind-turbine rotation period and the radar observation time (the burst duration of the Doppler radar). The initial case when the blades are rotating with $\Omega = 0.1$ Hz and radar measures Doppler spectrum using 128 pulses with PRF 1 kHz is shown in Fig. 8(a). Figure 8(b) represents a case when blades rotate ten times faster and radar uses the same settings as before. In this case for a better visual compatibility the sizes of wired-blades are decreased ten times to keep the maximum observed Doppler frequency constant. It is clear that a faster rotation during the same observation time makes micro-Doppler pattern smoother. Further increase of the

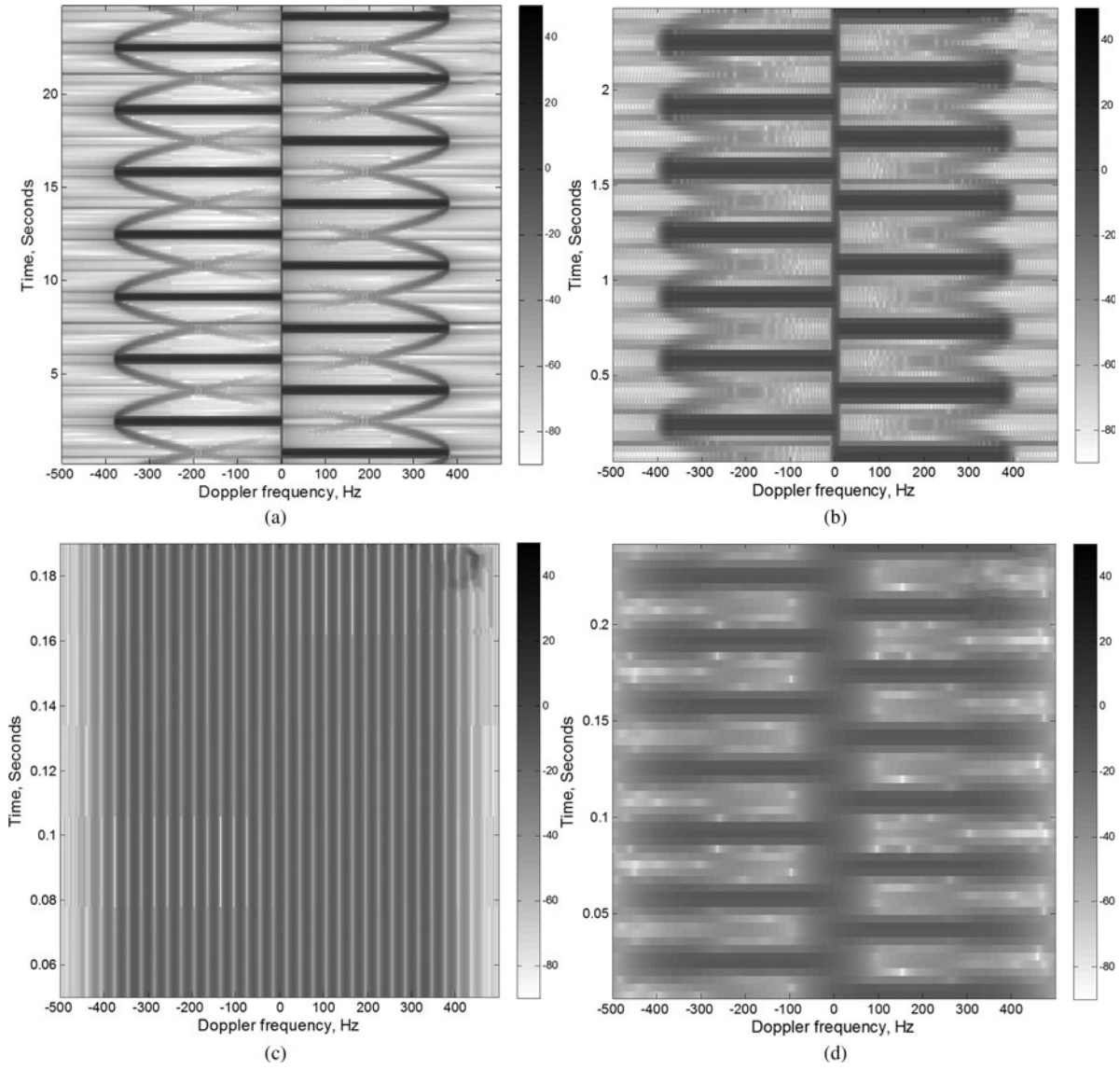

Fig. 8. Dependence of amplitude micro-Doppler patterns (in dB) from the relation between the rotation period of three-blades wind turbine and the radar's observation time.

blades rotation speed in ten times (and in ten times decrease of their lengths) for the fixed radar setting results (Fig. 8(c)) in the complete destruction of the Doppler pattern and conversion of the Doppler spectrum according to equation (13). Decreasing the radar observation time of such fast-rotating object in eight times (switching to burst length 16) restores the visibility of the micro-Doppler pattern (Fig. 8(d)) and returns the observables in the Doppler velocity domain.

These results, being supported with analytical derivations, give a method for optimal selection of the Doppler radar observation time for many types of rotating objects – not only wind turbines but also helicopters and propelled aircraft.

VI. DISCUSSION AND CONCLUSIONS

In this paper, we demonstrated the possibility to use the simplest linear wire structure for EM simulation of the wind-turbine Doppler temporal patterns. The proposed model does not take into account near-field effects, such as EM coupling between elements of simulated wired structure.

Despite of its simplicity, such a model provides reliable results, which are comparable with the real radar observations. We showed that the model developed can be used for initial analysis and interpretation of the influence of wind-turbine construction elements on the observed with radar micro-Doppler patterns.

The proposed model also gives a possibility to analyze analytically the important relation between the Doppler radar observation time (the time on target, dwell time) and the rotation period of any rotating target on the measured Doppler spectrum.

Further development of the proposed simulation approach can include the three-dimensional (3D) generalization of model's geometry, effects of the multiple scattering on construction elements, the shadowing effects, the multipath propagation and the polarimetric effects. It is clear that a

single wire, being polarization anisotropic target, could not describe the full variety of the observed polarimetric effects. To include them into consideration, the wire representation of orthogonal cuts of the 3D wind-turbines blade's construction can be analyzed.

ACKNOWLEDGEMENTS

The authors are very grateful to Fred van der Zwan and Etienne Goossens for their efforts in the PARSAX radar maintenance and data collections.

REFERENCES

[1] Kent, B.M.; Hill, K.C.; Buterbaugh, A.; Zelinski, G.; Hawley, R.; Cravens, L.; Tri-Van; Vogel, C.; Coveyou, T.: Dynamic radar cross section and radar Doppler measurements of commercial general electric windmill power turbines Part 1: predicted and measured radar signatures. IEEE Antennas Propag. Mag., **50** (2) (2008), 211–219.

[2] Ohs, R.R.; Skidmore, G.J.; Bedrosian, G.: Modeling the effects of wind turbines on radar returns, in Military Communications Conf. 2010 – MILCOM 2010, October 31 2010–November 3 2010, 272–276.

[3] Perry, J.; Biss, A.: Wind farm clutter mitigation in air surveillance radar. IEEE Aerosp. Electron. Syst. Mag., **22** (7) (2007), 35–40.

[4] Balanis, C.A.: Antenna Theory: Analysis and Design, Wiley, New York, 2005.

[5] Wind turbine Enercon E-82 E2/2300 kW. Web page http://www.enercon.de/en-en/63.htm, 05.01.2015

[6] Wind Turbine V90–3.0 MW VCS 50 Hz, General Specification, Vestas Wind Systems, Denmark, available on site vestas.com

[7] Krasnov, O.A.; Babur, G.P.; Wang, Z.; Ligthart, L.P.; van der Zwan, W.F.: Basics and first experiments demonstrating isolation improvements in the agile polarimetric FM-CW radar – PARSAX. Int. J. Microw. Wirel. Technol., **2** (2010), 419–428.

[8] Abramowitz, M.; Stegun, I.A.: Handbook of Mathematical Functions, with Formulas, Graphs, and Mathematical Tables, Dover Publications, New York, NY, 1970.

Oleg A. Krasnov received the M.S. degree in Radio Physics from Voronezh State University, Russia, in 1982, and the Ph.D. degree in Radiotechnique from the National Aerospace University "Kharkov Aviation Institute", Ukraine, in 1994. In 1999 Dr. Krasnov joined the International Research Center for Telecommunications and Radar (IRCTR), TU Delft. Since 2009 he has been a senior researcher at the Microwave Sensing, Signals and Systems (MS3) section of the Faculty of Electrical Engineering, Mathematics, and Computer Science (EEMCS) at Delft University of Technology, and became a Universitair Docent (Assistant Professor) there in 2012. His research interests include radar waveforms, signal and data processing algorithms for polarimetric radars and distributed radar systems, multi-sensor atmospheric remote sensing, optimal resource management of adaptive radar sensors, and distributed systems. Dr. Krasnov served as the Secretary of the 9th European Radar Conference (EuRAD'12), Amsterdam, the Netherlands.

Alexander G. Yarovoy graduated from the Kharkov State University, Ukraine, in 1984 with the Diploma with honor in Radio Physics and Electronics. He received the Candidate of Physical and Mathematical Sciences and Doctor of Physical and Mathematical Sciences degrees in Radio Physics in 1987 and 1994, respectively. In 1987 he joined the Department of Radiophysics at the Kharkov State University as a Researcher and became a Professor there in 1997. From September 1994 to 1996 he was with Technical University of Ilmenau, Germany as a Visiting Researcher. Since 1999 he is with the Delft University of Technology, the Netherlands. Since 2009 he leads there a chair of Microwave Sensing, Systems, and Signals. His main research interests are in ultra-wideband microwave technology and its applications (in particular, radars) and applied electromagnetics (in particular, UWB antennas). He has authored and co-authored more than 250 scientific or technical papers, four patents, and fourteen book chapters. He served as a Guest Editor of five special issues of the IEEE Transactions and other journals.